Sports Eng (2016) 19:219–227
DOI 10.1007/s12283-016-0194-x

ORIGINAL ARTICLE

Augmented inertial measurements for analysis of javelin throwing mechanics

Olli Särkkä[1] · Tuukka Nieminen[1] · Saku Suuriniemi[1] · Lauri Kettunen[1]

Published online: 28 January 2016

Abstract This paper examines the exploitation of inertial measurements to analyze javelin throwing mechanics. The main objective was to demonstrate that consumer-grade inertial navigation systems, augmented with some position and attitude data obtained from a video sequence, yield detailed information of the mechanics of javelin throwing. Especially, such a system makes it possible to analyze the momentary force and power exerted on the javelin during the acceleration phase. Although the presented system is a pilot, leaving space for further improvements, it already reveals the potential of inertial navigation systems to sports. In practise, an inertial measurement unit was embedded inside the tip of the javelin to determine the javelin's momentary attitude, position, and velocity. Graphs on the speed and angular velocity about the longitudinal axis of the javelin during the whole performance are presented. The maximum estimated release speed and release angular speed were 28.02 m/s and 215.9 rad/s, respectively. The acceleration phase trajectory of the javelin and its deviation from a straight line path are demonstrated. Additionally, the momentary forces and powers are shown and the effect of aerodynamic forces on the projectile is specified. The magnitude of the maximum tangential forces and accelerating powers were 364 N and 9.76 kW. The duration and length of the acceleration phase trajectory varied between 223 and 231 ms, and 2.48 and 2.75 m. To estimate the accuracy of the inertial measurements, the acceleration phase results were compared to measurements made with high-speed cameras.

✉ Olli Särkkä
olli.sarkka@gmail.com

[1] Department of Electrical Engineering, Tampere University of Technology, P.O. Box 692, 33101 Tampere, Finland

Keywords Time-parametrized trajectory · Force · Work · Power · Inertial navigation

1 Introduction

This paper studies the *mechanics of javelin throwing*. There is no straightforward approach to measure the run-up, acceleration, and flight phase of a javelin throw. The kinematics of the act has been studied in [5, 12, 22, 25], and javelin trajectories have been simulated in [11, 13]. Furthermore, extensive reviews about the biomechanics of javelin throwing can be found in [4, 16]. Yet little data are available about the kinetics.

For the above reason, an inertial measurement unit (IMU) and an analysis software system were developed to study javelin throwing. In addition it was sought to ascertain the extent to which modern technology and low-cost consumer-grade sensor systems could be exploited to analyze athletic throwing events.

A custom-made IMU was embedded in the tip of the javelin to enable measurement of the projectile's accelerations and angular velocities. From this data, the attitude and the time-parametrized trajectory of the javelin tip were determined. The motion of the rest of the javelin could be implicitly estimated from this data.

The following questions about javelin throwing were of special interest:

(a) How long is the acceleration phase?
(b) How long is the trajectory of the javelin's centre of mass during the acceleration phase?
(c) Is the trajectory of the centre of mass linear in the acceleration phase or do athletes accelerate the javelin along a curvilinear trajectory?

(d) What is the momentary force and power exerted on the javelin?
(e) How can one specify and what is the effect of the aerodynamic forces of the javelin during the flight?

Answers to (a)–(d) helped increase understanding of the limits of human performance, whereas an answer to (e) helped to focus on the effect of the projectile and the prevailing wind on the distance of the throw. In the tests, IMU measurements were designed to address questions (a)–(e), and to demonstrate the potential of modern technology.

2 The challenge of conducting a javelin inertial measurement

Measuring a javelin throw with an IMU requires at least gyroscopes and/or accelerometers, a data logger, a communication link, and a battery in the projectile. Furthermore, since the sensors are typically of a limited range, and since accelerations and angular velocities vary significantly between different phases, in practice several sensors with different measurement ranges must be used.

For instance, the best male athletes are known to accelerate a javelin up to a speed of about 31 m/s [17, 26]. The acceleration phase itself takes about 0.25 s, and thus the range of accelerations differs from those of the flight. In contrast, some athletes make the projectile spin rapidly during the flight, whereby the range of angular velocities then diverges widely from that at the beginning of the acceleration phase.

The rationale for embedding an IMU in the tip was, first, that the tip vibrates less than the centre of the javelin during the flight phase. Second, IMU sensors are located on a somewhat flexible circuit board. However, data analysis is significantly simpler, if the sensor system could be assumed rigid. Consequently, the tip turned out to be a good compromise. In addition, the effect of the IMU on the mechanical properties of the javelin was to be minimized. Furthermore, to operate the IMU, a power and a start switch and a USB port were needed for data transfer; hence it was practical to embed all this in a detachable metal tip.

The above setup made it possible to explicitly specify the time-parameterized trajectories of the javelin tip and, further, to explicitly determine its kinetics. A simple and straightforward approach to estimate the centre of mass trajectory is to assume that the javelin is a rigid body, as is done in this paper. On average, this approach is correct over each cycle of the javelin body vibration (more advanced techniques to specify the trajectory of the centre of mass with higher precision can be employed, but they are beyond the scope and space of this paper).

3 Mechanical principles of the acceleration phase

One goal was to examine the kinetics of the acceleration phase. For this reason, first the acceleration phase is specified and thereafter the basic mechanical principles are briefly revised.

In conventional high-speed camera measurements, the moment the athlete hits his/her forward foot on the ground has been interpreted as the beginning of the acceleration phase, and it ends when the athlete loosens his/her grip on the javelin [17, 26].

The javelin may, however, accelerate already before the forward foot contacts the ground, for example, if the athlete pushes him/herself forward with the back leg. Accordingly, in the sense of mechanics, the acceleration phase starts at the moment the tangential acceleration of the javelin is zero and ends at the moment when the tangential acceleration is zero again.

This is the specification adopted in this paper for the IMU measurements. Note that this specification implies that the tangential force, and thus also the translational power, is zero at the beginning and end of the acceleration phase and positive elsewhere.

In throwing a javelin, a high release speed is a necessary condition for a long throw. For this, the work that changes the translational kinetic energy of the javelin should be maximized. This work is the integral of the force that acts on the javelin along the trajectory where the projectile has moved from a stationary state to the moment of release. Obviously, the most of this work is done during the acceleration phase. In practice, the athlete tries to find a combination of force and trajectory length of the acceleration phase that maximizes the work.

In addition to the force, the *power* generated by muscles is also limited. Since translational power is the dot product of force and velocity, the higher the speed of the javelin, the smaller is the available force to further accelerate the projectile in the direction of the motion.

The acceleration of an object on which a force is exerted depends on the mass, and in the same fashion, the angular acceleration of an object on which a torque is exerted is inversely proportional to the moment of inertia.

4 Throwing techniques in the acceleration phase

In practice, to maximize the work into translational kinetic energy, the athlete pulls the javelin back and plants his/her front leg far ahead during the last stride(s). Thereafter, the available momentary force constrains the acceleration, and when the speed of the javelin is high enough, the power constrains the available momentary force. However, the

athlete can change the direction of motion despite the power limit by applying a normal force perpendicularly to the javelin trajectory. The corresponding momentary translational power is zero, because the normal force and velocity vector are perpendicular to each other.

The above means that the javelin can be accelerated not only in the direction of motion, but also by exerting a force "sideways", which makes the trajectory curve. In practice, this occurs when a larger set of muscles becomes active during the acceleration phase.

A force in the normal direction extends the acceleration phase trajectory. Consequently, if the available tangential force and power are the same as in the case of accelerating the javelin along a straight line, this results in a higher release speed. Or, conversely, the same release speed can be achieved with a smaller tangential force and power. However, accelerating the projectile along a curved trajectory is obviously a technical challenge.

5 Specifying the effect of the projectile and wind

In javelin throw, one tries to get the projectile as far as possible. However, the result depends not only on the athlete but also on the projectile and on the wind, which may change significantly even during a single competition or training session. This makes it difficult to distinguish between the effect of the projectile and the wind on the flight phase and throw distance.

However, if a javelin was thrown in a vacuum, the gravity would be the only force acting on the javelin during the flight phase. In such a case, the projectile is in *free fall*.

In real conditions, aerodynamic forces also act on the javelin. Thus, the aerodynamic forces manifest themselves in the difference between free fall and the actual flight trajectory. This difference is also precisely the data gathered from inertial sensors. Consequently, one may take sides on the properties of a projectile by comparing the actual flight trajectory to a hypothetical free fall, which is easily specified once the velocity of the javelin is known.

6 Measurements

The motion of a rigid body is characterized by six degrees of freedom (DOF): one may select three linearly independent translations and rotations. Accordingly, in inertial navigation, three linear accelerometers and three gyroscopes are often used to cover all the six DOFs [6]. Together with suitable models, the data gathered from such a sensor set makes it possible to estimate time-parametrized trajectories of rigid bodies.

A custom-made IMU of 17 cm by 2 cm and of mass 47 g with the battery was embedded in the tip of a javelin, about 0.70 m from the centre of mass (for details, see Fig. 1). In total, the IMU consisted of four gyroscopes and six accelerometers. In addition to one gyroscope [23] triad (measurement range ± 105 rad/s), a wide measurement range (± 350 rad/s) gyroscope [3] with its sensitive axis parallel to the long axis of the javelin was installed to cover the substantial longitudinal rotation of the javelin after release. Two accelerometer [1, 2] triads with different measurement ranges ($\pm 160\,\mathrm{m/s^2}$ and $\pm 1200\,\mathrm{m/s^2}$ respectively) were chosen to cover the wide range of accelerations experienced by the javelin during each throw. Accelerations and angular velocities were measured at a sampling rate of 1 kHz, and the measurement data was stored in the IMU flash memory. The javelin with its IMU fulfilled the IAAF regulations on mass (810 g), centre of mass (distance from metallic tip to centre of mass was 1.06 m), and dimension [14]. The metallic tip was lightened to compensate for the mass of the IMU. The moment of inertia about the longitudinal axis of the javelin was 0.00011 kg $\mathrm{m^2}$ and about the other two principal axes 0.47 kg $\mathrm{m^2}$.

In inertial navigation, the measurement accuracy depends on the chosen sensors. To improve the accuracy, the sensors were calibrated. The javelin was rotated 4π radians about each of its principal axis set to horizontal. From these data, the scale factors, biases, and misalignments of accelerometers and gyroscopes were estimated. To minimize the effect of any remaining temporal errors, the calibration was done just before every throw.

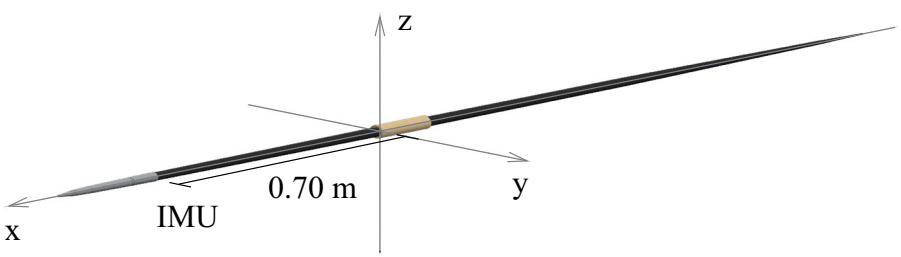

Fig. 1 Javelin with the IMU and the principal axes of inertia

6.1 Estimating attitude, velocity, and position

The attitude, velocity, and position of the IMU are solved from the measured acceleration and the angular velocity data. The technical details can be found in [18–21] and the main principles can be summarized as follows:

Assuming that the attitude λ and angular velocity ω of the javelin are known at a moment t_0, the attitude at $t_0 + \Delta t$ can be approximated. Consequently, if the attitude is known in the beginning of some interval and the angular velocity is sampled frequently enough, the attitude can be found over the whole interval. The process requires solution of a differential equation, and the accuracy of the solution tends to deteriorate over time. If the attitude is known at several times within the interval, the accuracy can be substantially improved.

Successive finite rotations of objects in three dimensions cannot be added together in an arbitrary order: the end attitudes usually depend on the order. Therefore, on the concrete level, successive rotations were expressed as (left) multiplications by direction cosine matrices $\Lambda(t)$ [8], which describe all rotations of a rigid body.

The orthogonality constraint $\Lambda^T\Lambda = \Lambda\Lambda^T = \mathbf{I}$ must not be violated, and this imples a constraint on the time derivative of Λ. Otherwise (left) multiplication by such matrix would not just rotate, but also deform and/or scale the object. Within this restriction the time derivative is

$$\dot{\Lambda}(t) = \Lambda(t)\Omega(t) \quad \forall \quad t \in [t_0, t_1], \tag{1}$$

$$\Omega(t) = \begin{bmatrix} 0 & -\omega_z(t) & \omega_y(t) \\ \omega_z(t) & 0 & -\omega_x(t) \\ -\omega_y(t) & \omega_x(t) & 0 \end{bmatrix}$$

where $\Omega(t)$ is the antisymmetric angular velocity tensor that consists of measured (Cartesian) components of the angular velocity vector $\boldsymbol{\omega}$ [24].

Solution of Eq. 1 as an initial value problem [7] makes measurement errors, noise in Ω, as well as inaccuracy of numerical computation, eventually accumulate. The inclusion of attitudes as constraints at several time instants alleviates the problem. In javelin throw, the initial and final attitude—the starting and landing attitude—constituted attitude constraints. While this can significantly improve the accuracy, it also transforms the initial value problem with a routine solution process to an over-determined boundary value problem. In over-determined problems, the quality of the solution depends on a weight between the attitude constraints and the differential equation. Technically, the weight was set with Tikhonov regularization [10].

In general, the solution of an over-determined system does not satisfy the Eq. 1 and attitude constraints exactly. The Eq. 1 at specific time instants can be reduced into a linear equation, whose residual is $\mathbf{r}_d$. Let $\mathbf{r}_c$ be the residual of linear equation stating the attitude constrains. The solution obtained with Tikhonov regularization problem is a matrix Λ_α containing all the direction cosine matrices of the time interval, defined by

$$\Lambda_\alpha = \underset{\Lambda}{\operatorname{argmin}} \left\{ \|\mathbf{r}_d(\Lambda)\|_F^2 + \alpha \|\mathbf{r}_c(\Lambda)\|_F^2 \right\}, \tag{2}$$

where $\|\cdot\|_F$ denotes the (Frobenius) norm [7]. The regularization parameter $\alpha > 0$ controls the weight between the residual norms. The greater the α, the more attitude constrains are weighted (trusted). Parameter value $\alpha = 10^3$ was used for the attitude computation to reflect the high confidence to attitude constrains.

Once the attitude is found over the desired interval, the position $\mathbf{p}$ and velocity $\mathbf{v}$ are solved in the same manner. They are subject to

$$\begin{cases} \dot{\mathbf{v}}(t) = \Lambda(t)\mathbf{a}(t) + \mathbf{g} \\ \dot{\mathbf{p}}(t) = \mathbf{v}(t), \end{cases} \tag{3}$$

where $\mathbf{a}$ is the acceleration given by the accelerometers and $\mathbf{g}$ is the gravity.

In javelin throwing, the starting position and velocity, landing position, and six positions of the run-up phase were gathered with two additional video cameras, constituting the position and velocity constrains. The first-order system in Eq. 3 together with the position constraints is similarly amenable to residual minimization with Tikhonov technique. To give high confidence to the position constrains, they were weighted with parameter value $\alpha = 10^2$.

6.2 High-speed camera measurements

To verify the accuracy achieved with the above measurement setup, the results were compared against an image sequence analysis made with two high-speed video cameras (independently of the above mentioned additional video cameras). In this analysis, a point of the object was tracked to estimate its trajectory. Image sequence analysis was made of the acceleration phase with the pair of cameras whose frame rate was 1000 fps. Markers were placed on both sides of the IMU sensors about 5 cm from sensors' position.

To calibrate the high-speed camera measurements, a rectangular metallic cuboid with known dimensions (approx. 2 m × 2 m × 3 m) was placed in the area of the acceleration phase. In total, 18 reference points of cuboid were used with a direct linear transformation (DLT) method to transform two-dimensional camera measurements to three-dimensional coordinates [9], and the results were low pass filtered at 20 Hz cut-off frequency to filter out the errors that follow from the manual process of

recognizing image pixels. Image sequence analysis was made with the Ariel Performance Analysis System® (APAS).

7 Results

From the measured acceleration and angular velocity data, a time-parametrized trajectory (equipped with attitude) was created to specify the javelin's position and velocity. From this, it was straightforward to calculate the javelin's translational and rotational kinetic energies, power, and angular acceleration. Unless otherwise stated, the results were calculated for the position of the IMU (Fig. 1).

An example of such a trajectory (throw 6 in Table 1) and the measurement set up is shown in Fig. 2. The trajectory is a reconstruction of the movements of the projectile. First, the athlete took the javelin from the stand and then walked to the beginning of the runway. After standing still for a moment, he started his run along the right side of the run-up area, accelerated, and released the javelin just before the throw arc line. The black lines present the attitude of the javelin, and they are plotted at 0.25 s intervals from the moment of release.

Table 1 The acceleration phase and the release parameters estimated using the IMU and the image sequence analysis (ISA)

Throw Athlete		1. A	2. B	3. B	4. A	5. A	6. A
l_t (m)		69.48	65.43	66.65	71.61	73.66	72.39
l_f (m)	IMU	64.49	67.29	66.94	72.03	74.08	73.71
l_a (m)	IMU	2.636	2.489	2.639	2.476	2.566	2.751
d (%)	IMU	2.07	3.19	4.29	2.91	3.05	2.94
t_a (s)	IMU	0.234	0.223	0.223	0.231	0.227	0.229
v_i (m/s)	IMU	6.28	5.21	6.02	5.16	5.48	5.56
v_r (m/s)	IMU	25.39	26.07	26.12	26.74	27.14	28.02
	ISA	26.53	25.68	26.25	26.95	27.36	27.42
α_r (deg.)	IMU	35.12	34.44	34.93	38.17	36.71	31.59
	ISA	35.51	33.66	32.44	36.00	38.99	34.72
α_a (deg.)	IMU	9.65	1.90	2.57	8.59	8.21	9.47
	ISA	5.98	2.79	3.10	5.83	2.59	8.31
α_y (deg.)	IMU	21.76	9.55	8.10	14.28	20.43	18.44
	ISA	13.85	12.75	10.46	12.57	18.11	17.90
ω_r (rad/s)	IMU	198.3	80.7	88.6	209.5	215.9	195.9
$F_{\max}$ (N)	IMU	300	258	226	279	364	315
$P_{\max}$ (kW)	IMU	7.59	5.07	5.06	5.72	9.76	8.77
Δl (m)	IMU	4.99	−1.86	−0.29	−0.42	−0.42	−1.32
Δv (m/s)	IMU	19.11	20.86	20.1	21.58	21.66	22.46

l_t is the length of the throw

l_f is the distance between throw arc line and the end of free fall trajectory calculated from the release position and velocity of the javelin

l_a is the length of the mass centre trajectory of the acceleration phase

d is the deviation of the length of the acceleration phase mass centre trajectory from a straight line

t_a is the duration of acceleration phase

v_i is the initial acceleration phase speed of the javelin

v_r is the release speed

α_r is the release angle

α_a is the angle of attack

α_y is the angle of yaw

ω_r is the release angular velocity about the longitudinal axis of the javelin

$F_{\max}$ is the magnitude of the maximum tangential force applied to the javelin during the acceleration phase

$P_{\max}$ is the maximum translational power during the acceleration phase

$\Delta l = l_t - l_f$

$\Delta v = v_r - v_i$

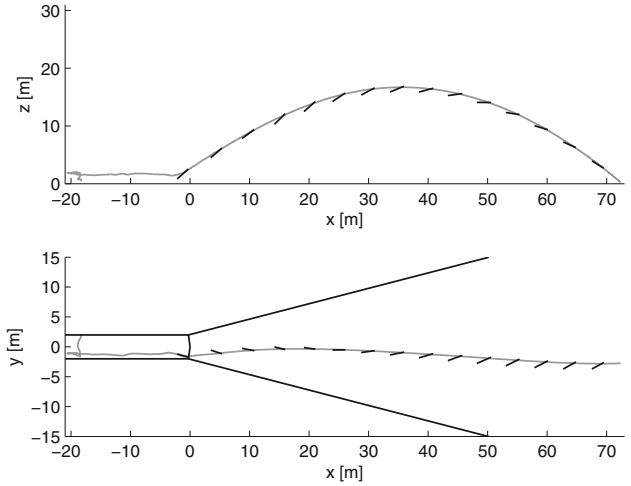

Fig. 2 An example of the trajectory of the javelin for the entire event. The attitude of javelin is shown in 0.25 s intervals during the flight phase

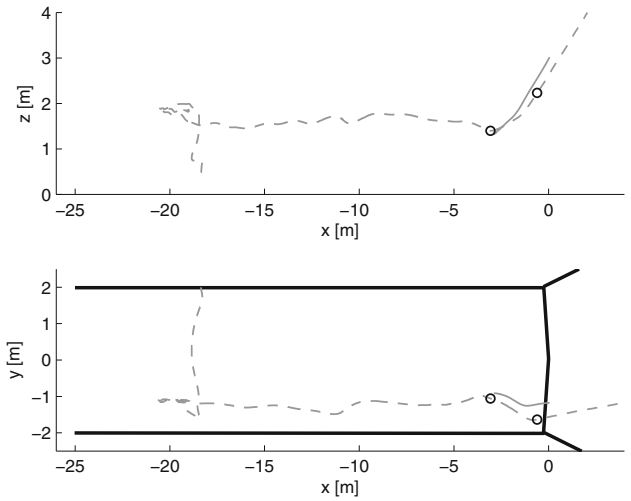

Fig. 3 A comparison of the trajectories of the runway measured with the IMU (*grey dash line*) and the high-speed camera (*grey solid line*). The beginning and the end of the acceleration phase is marked with *black circles*

The trajectory (grey solid line) of throw 6, generated with high-speed cameras tracking the position of the IMU, is shown in Fig. 3. The start and end points of the acceleration phase are marked with black circles. The momentary differences between the trajectories generated with the IMU and the high-speed cameras in the x, y, and z-direction never exceeded 0.39, 0.45, and 0.58 m, respectively. In other measured throws the momentary differences between trajectories varied maximally 0.41–0.91 m, 0.16–0.46 m, and 0.36–0.62 m.

To compare the time-parametrized trajectories, the IMU and the high-speed video measurements had to be

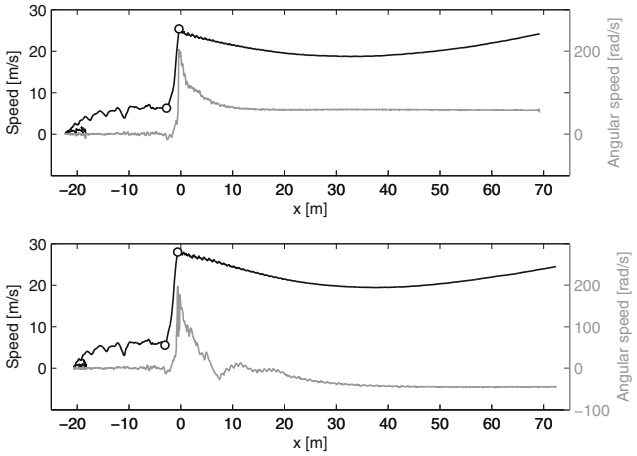

Fig. 4 The speed (*black line*) and angular velocity about the longitudinal axis of the javelin (*grey line*) of throws 1 (*top*) and 6 (*below*). The beginning and the end of the acceleration phase is marked with *black circles*

synchronized, which was done with a LED embedded in the tip of the javelin. Flash of the LED, which was synchronous with IMU measurements, was recorded by a high-speed camera with 200 Hz sample rate. Consequently, the maximum synchronization error was 5 ms. The synchronization error in position between the trajectories generated from IMU and video measurements depends on the velocity of the javelin; the higher the speed, the greater is the error. The maximum synchronization errors between the time-parametrized trajectories were 12, 2 and 8.5 cm in x, y, and, z-direction, respectively.

Figure 4 shows the speed (black line) and angular velocity (grey line) about the longitudinal axis of the javelin in throws 1 (top) and 6 (below). The acceleration phase is marked with black circles. During the flight phase, there was a notable difference between angular velocities. In throw 1, after a 10-m flight, the angular velocity about the longitudinal axis of the javelin was about 60 rad/s for the rest of the flight phase. In throw 6, after release, the angular velocity decreased and turned negative. In other words, at the end of the flight phase, the javelin rotated opposite to that at the moment of release.

Table 1 shows the acceleration phase and the release parameters of six throws made by two athletes. In image sequence analysis, the release parameters were estimated at the moment the athlete loosened his grip on the javelin, whereas in the case of the IMU, the parameters were calculated at the moment the tangential acceleration is zero. These two moments are not necessarily the same.

The estimated parameters were:

- The length of the throw and the free fall trajectory calculated from the release position and velocity.
- The length and duration of the acceleration phase centre of mass trajectory of the javelin.

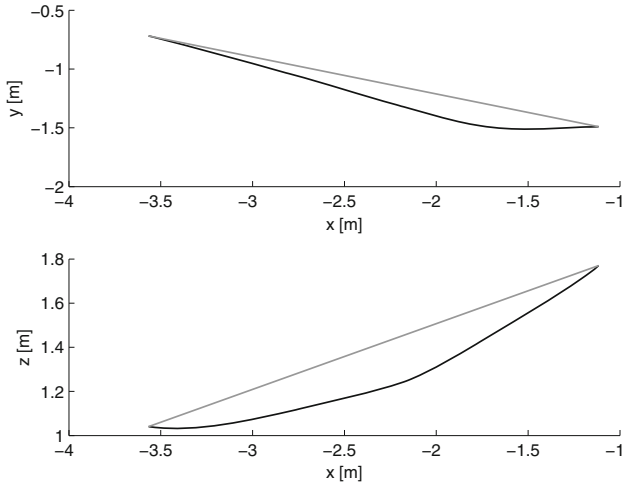

Fig. 5 The acceleration phase centre of mass trajectory (*black line*) of throw 6 and corresponding straight line path (*grey line*)

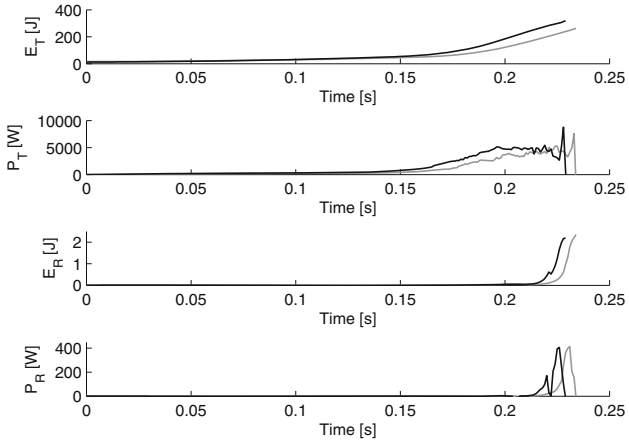

Fig. 6 In *top* the translational kinetic energy E_T and power P_T of the acceleration phase of throws 1 (*grey line*) and 6 (*black line*). Below the rotational kinetic energy E_R and power P_R of the acceleration phase of throws 1 and 6 about the longitudinal axis of the javelin

- The deviation of the centre of mass trajectory from a straight line.
- The initial and release speed of the acceleration phase.

In addition, the following angles were estimated; the release angle (the angle between the velocity of the javelin and the horizontal plane at the moment of release), the angle of attack (the angle between a vector parallel to the javelin and the horizontal plane minus the release angle), and the angle of yaw (the angle between a vector parallel to the javelin and the vertical plane minus the angle between the velocity of the javelin and the vertical plane at the moment of release). Furthermore, Table 1 shows the release angular velocity about the longitudinal axis of the javelin, the magnitude of the maximum tangential force applied to the javelin, and the maximum translational power.

According to Table 1, the acceleration phase centre of mass trajectories deviated in length from a straight line path by 2.07–4.29 %. In other words, both athletes accelerated the javelin along a longer curvilinear rather than a linear trajectory. The acceleration phase centre of mass trajectory (black line) versus the straight line path (grey line) of throw 6 is shown in Fig. 5.

The longest acceleration phase trajectory corresponds to the highest release speed. However, the release speed depends also on the force the athlete exerts on the javelin during the acceleration phase and the initial acceleration phase speed of the javelin. Extending the acceleration phase trajectory enables the athlete to increase the translational work done on the javelin while the tangential force component remains the same. This results in a higher release speed.

The translational kinetic energy and power in the acceleration phase of throws 1 and 6 are plotted at top of Fig. 6. In javelin throw, one should find a combination of power and duration of the acceleration phase that maximizes the work. This results in the greatest change in the translational kinetic energy of the javelin. The duration of the acceleration phase depends on both the power and length of the trajectory. Increasing the power while the trajectory remains unaltered decreases the duration of the acceleration phase.

In addition to translational work, the athlete does rotational work on the javelin. The rotational kinetic energy and power about the longitudinal axis of the javelin of throws 1 and 6 are plotted at bottom of Fig. 6. The rotational kinetic energy differed from zero only at the end of the acceleration phase and was only a few joules at the moment of release; this indicates little rotational work. However, during the flight phase, the angular velocity about the longitudinal axis, together with the external torque caused by the aerodynamic forces, make the javelin precess. This changes the orientation of its longitudinal axis [15]. Precession is difficult to measure with a single IMU, since the javelin also flexes and vibrates during the flight phase. For this reason, it is not practical to take sides on the amount of the precession.

The magnitude of the tangential (grey line) and normal force (black line) applied to the javelin during the acceleration phase of throw 6 are shown in Fig. 7. The athlete not only accelerated the projectile in the direction of velocity, but also applied a normal force perpendicular to velocity, caused the javelin to deviate from a straight line path. In this case, the normal force reached the maximum at the end of the acceleration phase.

Table 1 shows that the actual length of the throws deviate from −1.86 to 4.99 m from the distance between the throw arc line and the ends of the free fall trajectories

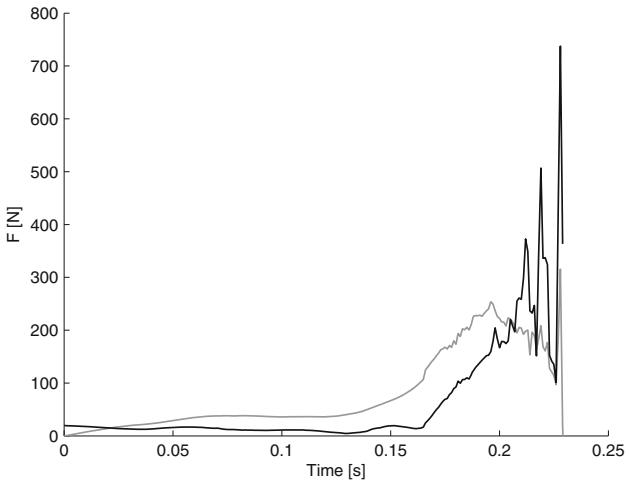

Fig. 7 The magnitude of the tangential force applied to the javelin (*grey line*) and the magnitude of the normal force (*black line*) during the acceleration phase of throw 6

calculated from the release velocities. In Fig. 8, the actual trajectories of throws 1 (69.48-m throw) and 6 (72.39-m throw) are plotted as seen from above, and the landing points of the javelin are marked with squares. Dots signify the end points of the free fall trajectories calculated from the release position and velocity. In free fall, gravity is the only force acting on the javelin. The paths between the dots and squares are free fall projections from the positions and the velocities of the javelins on their actual trajectories. Accordingly, the lines on the field demonstrate the effect of aerodynamic forces on the throw distance during the flight phase. During the measurement session, the wind blew in gusts; hence the difference between the end points of the free fall trajectories and the actual landing point depends not only on projectile properties (volume, shape, and moment of inertia), but also on external conditions.

8 Conclusions

This paper demonstrated that consumer-grade inertial measurements system augmented with some data obtained from a video sequence can be successfully exploited to estimate the attitude, position, and velocity of the javelin from the run-up to the instant of landing. In addition, the mechanics of the acceleration phase was analyzed in further details demonstrating that the data of such a measurement system can be employed to analyze differences between throwing techniques.

In the test session, the maximum observed momentary tangential force and power were 364 N and 9.76 kW, respectively, with a test javelin that fulfills all IAAF regulations.

Each athlete has a unique throwing technique. The inertial data can be employed to study such differences. The release speed depends mainly on the mechanical work done during the acceleration phase. Since work is the cumulative force along a path, the same release speed can be achieved on average with a smaller force, if the trajectory becomes longer. In the tests the athletes accelerated the javelin along a trajectory having a length that deviates 2.07–4.29 % from a straight line path.

The aerodynamic effects on the projectile during the flight was worked out by specifying the difference between the actual flight trajectory and the parabolic Newtonian free fall. The difference between actual throw lengths and the free fall estimations of the throws of the test session varied

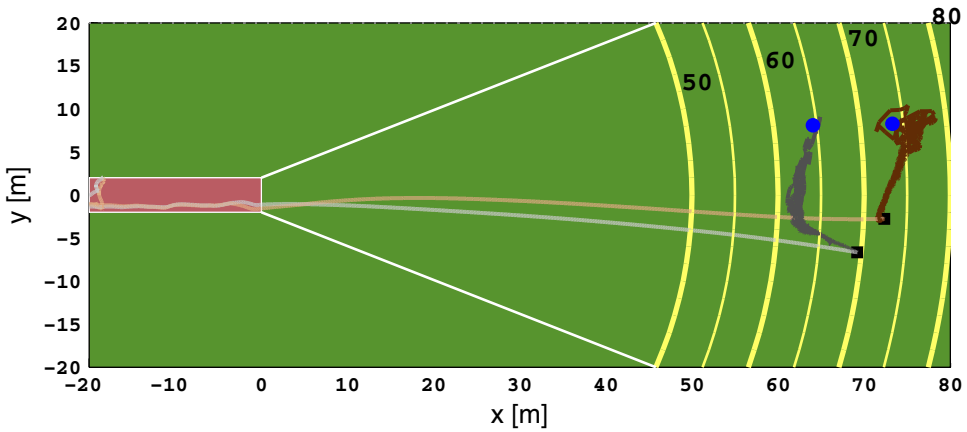

Fig. 8 The actual trajectories of throw 1 and 6 are calculated from the moment the javelin is taken from the stand to the instant of landing. The *dots* are the ends of the free fall trajectories calculated from the release position and velocity of the projectile. The paths from the *dots* are obtained by updating the free fall predictions during the projectile's flight, and the *squares* are the actual landing points. In both cases the free fall calculations reveal an effect of a side wind

from −1.86 to 4.99 m, suggesting a rather significant aerodynamic effect on the projectile.

Acknowledgments The authors thank the Research Institute for Olympic Sports, Riku Valleala, Simo Ihalainen, and Sami Kuitunen who shot and made the acceleration phase image sequence analysis, and Antti Nikkola who modelled the javelin with CAD system and calculated the principal moments of inertia of the javelin. There are no conflicts of interest to disclose. The Javelin bodies for this study were given by Nordic Sport, Sweden. Two elite javelin throwers volunteered to take part in this study. Both gave their written informed consent to participate in this study, and the experimental study protocol was approved by the chair of the Ethics Committee of Tampere University of Technology, Tampere, Finland.

References

1. Analog Devices (2009) ADXL326 Datasheet. http://www.analog.com/static/imported-files/data_sheets/ADXL326. Accessed 22 December 2015
2. Analog Devices (2010) ADXL193 Datasheet. http://www.analog.com/static/imported-files/data_sheets/ADXL193. Accessed 22 December 2015
3. Analog Devices (2010–2012) ADXRS649 Datasheet. http://www.analog.com/static/imported-files/data_sheets/ADXRS649. Accessed 22 December 2015
4. Bartlett RM, Best RJ (1988) The biomechanics of javelin throwing: a review. J Sports Sci 6:1–38. doi:10.1080/02640418808729791
5. Best RJ, Bartlett RM, Morriss CJ (1993) A three-dimensional analysis of javelin throwing technique. J Sports Sci 11:315–328. doi:10.1080/02640419308730001
6. Chatfield AB (1997) Fundamentals of high accuracy inertial navigation: introduction. American Institute of Aeronautics and Astronautics, Reston
7. Eldén L, Wittmeyer-Koch L, Nielsen HB (2004) Introduction to numerical computation—analysis and MATLAB® illustrations. Studentlitteratur, Lund
8. Farrell JA, Barth M (1999) The global positioning system and inertial navigation. McGraw-Hill, New York
9. Griffiths IW (2006) Principles of biomechanics and motion analysis. Lippincott Williams & Wilkins, Baltimore
10. Hansen PC (1998) Rank-deficient and discrete Ill-posed problems: numerical aspects of linear inversion. SIAM, Philadelphia
11. Hubbard M (1984) Optimal javelin trajectories. J Biomech 17:777–787. doi:10.1016/0021-9290(84)90108-8
12. Hubbard M, Alaways LW (1989) Rapid and accurate estimation of release conditions in the javelin throw. J Biomech 22:583–595. doi:10.1016/0021-9290(89)90010-9
13. Hubbard M, Rust HJ (1984) Simulation of javelin flight using experimental aerodynamic data. J Biomech 17:769–776. doi:10.1016/0021-9290(84)90107-6
14. IAAF (2014–2015) Competition Rules 2014–2015. http://www.iaaf.org/about-iaaf/documents/rules-regulations. Accessed 6 February 2015
15. Mansfield M, O'Sullivan C (2004) Understanding physics, 2nd edn. John Wiley & Sons Ltd, New York
16. Morriss C, Bartlett R (1996) Biomechanical factors critical for performance in the men's javelin throw. Sports Med 21:438–446. doi:10.2165/00007256-199621060-00005
17. Murakami M, Tanabe S, Ishikawa M, Isolehto J, Komi PV, Ito A (2006) Biomechanical analysis of the javelin at the 2005 IAAF World Championships in Athletics. New Stud Athl 21:67–80
18. Nieminen T (2013) A Non-recursive solution method for fixed-interval smoothing problems applied to short-term inertial navigation. Doctoral dissertation, Tampere University of Technology, pp 1–68
19. Nieminen T, Kangas J, Kettunen L (2011) Use of Tikhonov regularization to improve the accuracy of position estimates in inertial navigation. Int J Navig Obs. doi:10.1155/2011/450269
20. Nieminen T, Kangas J, Suuriniemi S, Kettunen L (2010) Accuracy improvement by boundary conditions for inertial navigation. Int J Navig Obs. doi:10.1155/2010/869127
21. Nieminen T, Kangas J, Suuriniemi S, Kettunen L (2014) Non-recursive fixed-interval smoothing-based approach to attitude estimation. IEEE Trans Aerosp Electron Syst 50:1884–1898. doi:10.1109/TAES.2014.120027
22. Saratlija P, Zagorac N, Babić V (2013) Influence of kinematic parameters on result efficiency in javelin throw. Coll Antropol 37:31–36
23. STMicroelectronics (2009) LPY4150AL Datasheet. http://www.st.com/st-web-ui/static/active/en/resource/technical/document/datasheet/CD00254147. Accessed 22 December 2015
24. Titterton DH, Weston JL (2004) Strapdown inertial navigation technology, 2nd edn. The American Institute of Aeronautics and Astronautics, Reston
25. Viitasalo J, Mononen H, Norvapalo K (2003) Release parameters at the foul line and the official result in javelin throwing. Sports Biomech 2:15–34. doi:10.1080/14763140308522805
26. Zatsiorsky V (2000) Biomechanics in sport: performance enhancement and injury prevention. Blackwell Science Ltd, Oxford